Regional brain volumetric changes despite 2 years of treatment initiated during acute HIV infection

Kalpana J. Kallianpur[a], Neda Jahanshad[b], Napapon Sailasuta[a], Khunthalee Benjapornpong[c], Phillip Chan[c], Mantana Pothisri[d], Netsiri Dumrongpisutikul[d], Elizabeth Laws[a], Lishomwa C. Ndhlovu[a], Katherine M. Clifford[e], Robert Paul[f], Linda Jagodzinski[g], Shelly Krebs[g,h], Jintanat Ananworanich[a,g,h], Serena Spudich[i], Victor Valcour[e], on behalf of the SEARCH010/RV254 Study Group

Objective: To assess changes in regional brain volumes after 24 months among individuals who initiated combination antiretroviral therapy (cART) within weeks of HIV exposure.

Design: Prospective cohort study of Thai participants in the earliest stages of HIV-1 infection.

Methods: Thirty-four acutely HIV-infected individuals (AHI; Fiebig I–V) underwent brain magnetic resonance (MR) imaging and MR spectroscopy at 1.5 T and immediately initiated cART. Imaging was repeated at 24 months. Regional brain volumes were quantified using FreeSurfer's longitudinal pipeline. Voxel-wise analyses using tensor-based morphometry (TBM) were conducted to verify regional assessments. Baseline brain metabolite levels, blood and cerebrospinal fluid biomarkers assessed by ELISA, and peripheral blood monocyte phenotypes measured by flow cytometry were examined as predictors of significant volumetric change.

Results: Participants were 31 ± 8 years old. The estimated mean duration of infection at cART initiation was 15 days. Longitudinal analyses revealed reductions in volumes of putamen ($P < 0.001$) and caudate ($P = 0.006$). TBM confirmed significant atrophy in the putamen and caudate, and also in thalamic and hippocampal regions. In exploratory post-hoc analyses, higher baseline frequency of P-selectin glycoprotein ligand-1 (PSGL-1)-expressing total monocytes correlated with greater caudate volumetric decrease ($\rho = 0.67$, $P = 0.017$), whereas the baseline density of PSGL-1-expressing inflammatory ($CD14^+CD16^+$) monocytes correlated with putamen atrophy ($\rho = 0.65$, $P = 0.022$).

Conclusion: Suppressive cART initiated during AHI may not prevent brain atrophy. Volumetric decrease appears greater than expected age-related decline, although examination of longitudinal change in demographically similar HIV-uninfected Thai individuals is needed. Mechanisms underlying progressive HIV-related atrophy may include early activation and enhanced adhesive and migratory capacity of circulating monocyte populations.

AIDS 2020, **34**:415–426

Keywords: acute HIV infection, biomarkers, brain atrophy, caudate, metabolites, monocytes, putamen

[a]University of Hawaii at Manoa, Honolulu, Hawaii, USA, [b]University of Southern California, Marina del Rey, California, USA, [c]SEARCH Thailand, Thai Red Cross AIDS Research Centre, Bangkok, Thailand, [d]Chulalongkorn University Medical Center, Bangkok, Thailand, [e]University of California at San Francisco, San Francisco, California, USA, [f]University of Missouri at St. Louis, St. Louis, Missouri, USA, [g]Walter Reed Army Institute of Research, Silver Spring, Maryland, USA, [h]Henry M. Jackson Foundation, Silver Spring, Maryland, USA, and [i]Yale University, New Haven, Connecticut, USA.

Correspondence to Kalpana J. Kallianpur, John A. Burns School of Medicine, 651 Ilalo Street, BSB 231, Honolulu, HI 96813, USA.
E-mail: kalpana@hawaii.edu
Received: 3 April 2019; revised: 3 October 2019; accepted: 12 October 2019.

DOI:10.1097/QAD.0000000000002436

ISSN 0269-9370

Introduction

The neuroimaging signature of chronic HIV infection includes gray and white matter atrophy [1–3], disrupted frontostriatal functional connectivity [4,5], and abnormal white matter structural connectivity patterns [6]. Many neuroHIV studies have included participants with advanced disease or severe immune compromise prior to treatment [7–10]. However, reductions in total and cortical gray matter (GM) volumes have been identified even during primary HIV infection (PHI, <1 year post-transmission) [11], and decreased brain parenchymal volume was observed within the first 100 days [12]. Initial brain alterations may be determined by the severity of immunosuppression [13].

Early initiation of combination antiretroviral therapy (cART) is associated with greater probability of restoring normal $CD4^+$ cell counts [14,15] and appears protective. Neurofilament light protein – a marker of ongoing HIV-related neurodegeneration [16] – is elevated in cerebrospinal fluid (CSF) during untreated PHI [17], but is normal after 6 months of cART initiated during acute HIV infection (AHI) [18]. Treatment that is implemented within 6 months of infection greatly decreases $CD4^+$ T-cell activation, and HIV DNA and RNA reservoir size [19,20]. The HIV DNA reservoir in peripheral blood mononuclear cells (PBMCs), established early in infection [21], predicts HIV disease progression and the time to viremic rebound following cessation of cART [22,23]. We and others have shown that peripheral monocytes harboring HIV in the setting of chronic HIV infection, and monocyte phenotypic changes associated with migration and activation, are linked to a range of brain abnormalities that persist, despite therapy [24]. Plasma elevations of soluble CD163 (sCD163) in PHI correlate with the proportion of $CD14^+CD16^+$ monocytes and decrease with effective cART [25]. Similar changes have been observed in AHI [26].

HIV invasion of the central nervous system (CNS) occurs early. The virus has been isolated in the brain 15 days after iatrogenic HIV infection, only 1 day after it was first found in blood [27]. Computational modeling of clinical data has identified the first 3 weeks postinfection as a window of opportunity in which cART initiation may optimally control HIV replication and prevent immune activation, and the establishment of viral reservoirs [28]. Whether HIV-induced brain injury can be arrested or slowed by immediate treatment remains unknown. SEARCH010/RV254 – a longitudinal cohort study of AHI – enrolls and evaluates participants 2–3 weeks following history of exposure. Thereafter, cART is commenced at once. Matched samples at baseline and 2-year follow-up are a strength of this study.

The present work evaluated SEARCH010/RV254 participants for changes in volumes of nine a priori brain regions of interest after 24 months of cART. Although HIV-infected individuals over age 60 have exhibited progressive brain atrophy despite more than 3 years of viral suppression [29], previous longitudinal studies suggest that early cART may prevent such injury. In a PHI cohort (infected for ~3.7 months and followed for up to 6 years), duration of untreated infection correlated with brain volume loss prior to cART initiation; however, after cART, no further atrophy was observed [30]. Two-year changes in subcortical volumes of aviremic chronically HIV-infected individuals on cART were comparable to those of HIV-negative controls, although the HIV+ group had smaller volumes [31,32]. We therefore hypothesized the absence of HIV-related brain atrophy; namely, volumetric loss beyond that attributable to normal aging, which in the SEARCH010/RV254 cohort would be small. The link between brain atrophy in chronic, stable HIV disease and a history of immunosuppression supports our conjecture that very early antiretroviral intervention may prevent brain damage [33].

Brain volume deficits have been associated with disrupted levels of cerebral metabolites [33] and plasma cytokines [34] in chronic HIV infection. Plasma neopterin – a marker of immune activation – correlates with peripheral blood HIV DNA burden [35], which, in turn, relates to HIV-associated brain injury [36] and cognitive disorders [35]. Soluble CD14 (sCD14) is a marker of monocyte activation [37]; high plasma sCD14 levels predict morbidity and mortality in HIV [38]. CSF concentrations of the neuronal injury marker S100B may be elevated in HIV-infected individuals [39] and, in Alzheimer's disease, correlate with brain atrophy [40]. Brain inflammation at baseline in the SEARCH010/RV254 cohort has been identified by magnetic resonance spectroscopy (MRS) and by elevated CSF levels of inflammatory markers such as neopterin [41,42]. The present work investigated baseline brain metabolites as predictors of volumetric changes found to be significant. Exploratory analyses examined plasma and CSF biomarkers, and monocyte phenotypes potentially implicated in HIV neuropathogenesis, for their predictive value.

Methods

Participants

Our study sample was drawn from the first 38 AHI enrollees with MRI in the SEARCH010/RV254 study in Bangkok, Thailand (ClinicalTrials.gov #NCT00796146) [41,43]. Participants were above 18 years of age, had confirmed acute HIV-1 infection, were cART-naive, and consented to initiating protocol-defined cART. Testing was performed to categorize them into Fiebig stages I–V by a hierarchical algorithm from pooled nucleic acid, HIV RNA, sequential immunoassay, p24

antigen, and western blot testing [44]: Fiebig I (RNA+, p24 antigen−), Fiebig II (p24 antigen+, IgM−), Fiebig III (IgM+, Western blot−), Fiebig IV (Western Blot indeterminate), and Fiebig V (Western Blot+ without p31) [45]. Neurologic interviews and examinations were performed by physicians at study entry and longitudinally, using tools developed by the AIDS Clinical Trials Group [46]. Treatment was initiated immediately after baseline evaluations. Exclusion criteria for this substudy were excessive motion on MRI and poor cART adherence resulting in plasma HIV RNA (viral load >200 copies/ml at 24 months). One individual who chose not to start treatment soon after entry was dropped from analysis. Two were excluded because of poor image quality and one because of high 24-month viral load, yielding a study sample of 34 with baseline and 2-year follow-up data (baseline MRI dates: 5/15/2009–11/2/2012). Antiretroviral combinations consisted of efavirenz, tenofovir, and emtricitabine (standard cART), with 20 of the 34 participants randomly assigned to receive additional maraviroc and raltegravir (cART intensification, or 'mega-cART') during the first 24 weeks. Viral load was also assessed at intermediate time-points (weeks 4, 12, 24, 36, 48, and 72 post-baseline).

All participants underwent hepatitis C antibody testing, blood Treponema pallidum hemagglutination assay (TPHA), and either Venereal Disease Research Laboratory (VDRL) or Rapid Plasma Reagin (RPR) testing (hereafter denoted as VDRL). Presence of chlamydia or gonorrhea was determined by clinical evaluation. Syphilis and treatment history were collected through interviews conducted by research physicians at enrollment. Syphilis (at the time of AHI) was defined by positive TPHA and VDRL in the absence of prior syphilis treatment.

Information on substance use was obtained for most participants by physician interviews conducted informally at study entry. Participants were asked whether they had used any illicit substance during the 4 months prior to enrollment. Those who responded affirmatively were questioned about their use, within the same period, of substances including cannabis, poppers (inhaled nitrites), amphetamines (with street names such as speed, whizz, and base), and methamphetamine (crystal meth, ice, glass, tina).

The study was approved by institutional review boards of the participating sites. All participants provided signed written consent.

Neuroimaging data acquisition and processing

Anatomical MRI data at both time-points were acquired by an axial 3D T1-weighted spoiled gradient echo image (3D SPGR, TE = 7 ms, TR = 11.2 ms, flip angle = 25°, with 1 mm voxel resolution) on a GE Signa HDx 1.5T clinical scanner (GE Healthcare, Milwaukee, Wisconsin, USA; software version 12-M4) using an 8-channel head coil for data reception and a standard body coil for transmission. Single-voxel MRS was performed using a double spin echo data acquisition (PROBE-P) with TE = 35 ms, TR = 1.5 s at four locations: left frontal white matter (FWM, 8 cc), midline frontal gray matter (FGM, 8 cc), occipital gray matter (OGM, 8 cc), and basal ganglia (12 cc) [42]. At the end of each scan, single-voxel MRS was conducted on a standard spectroscopy phantom (GE Healthcare) to verify scanner stability [42,47]. MRI/MRS data acquisition and quality assurance were performed by an experienced technician.

To obtain regional brain volumes, T1-weighted MRI data at baseline (month 0, or M0) and month 24 (M24) were processed using the longitudinal pipeline [48] of the FreeSurfer image analysis suite (http://surfer.nmr.mgh.harvard.edu/, v.5.3) [49]. Quality assurance of the FreeSurfer-derived volumes was performed by visual inspection of cortical and subcortical segmentations. Manual corrections were applied when necessary and were followed by reprocessing – a method that improves gray/white segmentation [50]. Total volumes of regions of interest (caudate, putamen, pallidum, thalamus, hippocampus, amygdala, nucleus accumbens, cortical gray matter, and cerebral white matter) were computed by summing over left and right brain hemispheres. Baseline MRS data were processed, and levels of N-acetylaspartate (NAA), choline (Cho), creatine, myoinositol, and glutamate-glutamine (Glx) quantified as previously reported [42].

Viral load measurements

HIV-1 RNA (viral load) was measured in M0 and M24 paired plasma and CSF samples using the Roche Amplicor HIV-1 Monitor, Test v1.5 or the Roche COBAS AmpliPrep/COBAS TaqMan HIV-1 Test, v2.0 (Roche Diagnostics, Branchburg, New Jersey, USA); the lower limits of plasma viral load detection were 50 and 20 copies/ml, respectively. The lower limit of detection of CSF HIV RNA was 80 copies/ml.

Clinical and biological markers and monocyte populations

Risk factors for HIV-associated cognitive impairment and/or decreased brain volumes include high plasma and CSF HIV RNA [7]; low $CD4^+$ cell count (especially nadir) [7,51]; and elevated plasma sCD163 [52] and cytokines tumor necrosis factor-alpha (TNF-α), interleukin (IL)-1β, IL-6, MCP-1, and IP-10 [34]. To identify factors that may help to preserve or monitor brain integrity, we assessed biomarkers measured in plasma and CSF (neopterin, sCD14, sCD163, IL-6, IL-1β, TNF-α, MCP-1, IP-10); and CSF S100B protein, a marker of astrocytic activation seldom studied in HIV. Also examined were monocyte subpopulations classified by CD14 and CD16 expression: classical ($CD14^+CD16^-$), intermediate/inflammatory ($CD14^+CD16^+$), and non-classical/patrolling ($CD14^{low}CD16^+$). These subsets were further analyzed for expression of CCR2,

CCR5, CX3CR1, P-selectin glycoprotein ligand-1 (PSGL-1), and CD163.

Levels of soluble biomarkers were assessed in plasma at months 0 and 24 for all participants, and for CSF when available, because not all participants elected to undergo the lumbar puncture procedure. Multiplex Luminex array was used to measure TNF-α, IL-1β, IL-6, MCP-1, S100B (CSF only) (Millipore, Burlington, Massachusetts, USA) and sCD163 (BioRad, Hercules, California, USA). Standard ELISA assays measured neopterin (GenWay Biotech, San Diego, California, USA), and sCD14 (R&D Systems, Minneapolis, Minnesota, USA). Monocyte phenotyping based on CD14, CD16, CCR2, CCR5, CX3CR1, PSGL-1, and CD163 expression was assessed by flow cytometry, and is described elsewhere [26,53]. All data were analyzed by Prism 6.0 (GraphPad, La Jolla, California, USA) using a four-parameter fit standard curve.

Statistical analysis

Wilcoxon signed-rank tests assessed regional volumetric changes from baseline (M0) to 24 months (M24). A Holm–Bonferroni correction for multiple comparisons was applied [54]. For each participant, we computed percentage volume change from baseline: that is, $(M0 - M24)/M0 \times 100$. Wilcoxon signed-rank tests also evaluated changes in neuronal and inflammatory markers, and the glial marker S100B, from baseline to 24 months for individuals who had data at both time-points. Univariate relationships between variables were assessed by Pearson or Spearman correlation, as appropriate.

For each brain region showing significant volumetric change, Spearman correlation was used to examine associations of baseline brain NAA, Cho, myoinositol, and Glx concentration ratios over creatine with percentage volume change. Statistical significance was defined by P less than 0.05. Additionally, volumetric changes were investigated in relation to baseline plasma and intrathecal inflammatory markers, and to baseline monocyte subsets; these analyses were exploratory as the predictor data were available only for participant subsets, limiting statistical power. SPSS V.23.0 (SPSS Inc., Chicago, Illinois, USA) was used.

Tensor-based morphometry

Longitudinal tensor-based morphometry (TBM) was performed as in Nir *et al.* [1], using ANTS registration software [55].

Results

Participant characteristics

After quality control, we evaluated 34 acute HIV participants (29 men) with median (range) age 29.0 (18–48) years; estimated time since exposure 15 (4–32) days; $CD4^+$ cell count 398 (132–1127) cells/μl; plasma viral load 5.52 (2.78–7.49) $\log_{10}$ copies/ml; and who were at Fiebig stages I ($n = 12$), II ($n = 2$), III ($n = 17$), IV ($n = 2$), and V ($n = 1$) at baseline. Demographic and clinical characteristics of the study sample at baseline and 24 months are summarized in Table 1. Optional CSF sampling was performed at study entry on 25 of the 34 participants.

At M0, the sample included one case of untreated systemic syphilis without neurosyphilis, one case of gonorrhea, and no cases of chlamydia. One individual was co-infected with the hepatitis C virus (HCV), which was not treated. The participant who had syphilis showed an elevated CSF white blood cell count at baseline; following systematic treatment, CSF white blood count levels returned to normal at week 24. Neurosyphilis was deemed unlikely as the individual was neuroasymptomatic and remained so. The participant with gonorrhea was treated immediately.

Data on illicit substance use were unavailable for three individuals, but the majority of our cohort ($n = 21$, or 68%) denied use within the 4 months prior to baseline. Ten participants reported using illicit substances during that time: poppers ($n = 4$); methamphetamine ($n = 3$); poppers and methamphetamine ($n = 2$); and no specific substance information ($n = 1$; only 'illicit drug use' was noted).

Clinical variables and inflammatory markers at baseline and follow-up

Plasma and CSF viral load decreased from M0 to M24, while $CD4^+$ cell count increased (Table 1). Decreases were seen in plasma and CSF neopterin, with median reductions from baseline of 33.1 and 59.1%, respectively. IP-10 levels dropped by 84.6% (in plasma) and 59.2% (CSF). Plasma sCD14, plasma IL-1β, and CSF TNF-α decreased also. Among the 10 participants who had CSF S100B data at both time-points, CSF S100B showed a nonsignificant increase (median 970.3–988.6 pg/ml; $P = 0.11$).

Review of data at weeks 4, 12, 24, 36, 48, and 72 showed that plasma viral load first dropped to less than 50 copies/ml at week 4 in 8 participants, week 12 in 15, week 24 in 9, and week 36 in 2. We note that 94% of cases had suppressed viremia by the 24-week follow-up. All participants were fully suppressed by week 36 and all remained aviremic after achieving suppression. The median [interquartile range (IQR)] time to suppression of plasma viral load to below 50 copies/ml was 12 (6–12) weeks in participants on mega-cART vs. 18 (10–24) weeks in those on standard cART ($P = 0.17$).

Regional brain volumetric changes after 24 months of combination antiretroviral therapy

Volumetric reductions were observed in the putamen ($P < 0.001$) and caudate ($P = 0.006$) over the first 24

Table 1. Characteristics [mean ± SD, median (minimum − maximum), or *n*] of study population.

Demographic/clinical variables	Month 0 (baseline)	Month 24	*P* value
n	34	34	–
Sex, # male (%)	29 (85%)	–	–
Age (years)	31.2 ± 8.3	–	–
Education (years)	16.4 ± 4.0	–	–
Duration of HIV infection (days)	15 (4–32)	–	–
$CD4^+$ cell count (cells/μl)	397.5 (132.0–1127.0)	644.5 (378.0–1200.0)	<0.001
Plasma HIV RNA (copies/ml)	333 971 (604–30 811 000)	50 (20–58)	<0.001
CSF HIV RNA (copies/mL)	1102 (0–201 803)[b]	0 (0–0)[c]	0.001[c]
Used illicit substance(s) in past 4 months, # (%)	10 (32%)[a]		
Co-infections, # (%)			
Hepatitis C	1 (3%)	–	–
Syphilis	1 (3%)	–	–
Gonorrhea	1 (3%)	–	–
Chlamydia	0 (0%)	–	–
Plasma markers			
sCD14 (pg/ml)	1 552 748 (724 106–2 324 882)	1 106 143 (765 350–1 955 069)[d]	<0.001[d]
sCD163 (pg/ml)	99 402 (19 895–377 504)[d]	85 525 (13 564–380 705)[e]	0.21[d]
Neopterin (pg/ml)	2510.8 (227.1–8895.4)	1399.4 (380.3–6889.9)[f]	0.001[f]
IL-6 (pg/ml)	0.43 (0.10–3.14)	0.25 (0.11–3.42)	0.68
IL-1β (pg/ml)	2.03 (0.48–12.59)[g]	1.50 (0.48–5.83)[h]	0.014[h]
TNF-α (pg/ml)	1.46 (0.17–9.10)	1.05 (0.17–75.82)	0.17
MCP-1 (pg/ml)	273.2 (62.2–1781.9)	352.8 (108.9–1145.1)[d]	0.86[d]
IP-10 (pg/ml)	2821.8 (33.4–13 924.0)	446.7 (160.9–1616.9)[d]	<0.001[d]
Cerebrospinal fluid (CSF) markers			
S100B (pg/ml)	983.3 (622.3–1795.0)[i]	1027.2 (807.6 –1590.2)[j]	0.11[k]
sCD14 (pg/ml)	45 601 (2057–178 139)[h]	58 690 (25 000–1 516 912)[l]	0.83[j]
CD163 (pg/mL)	7157.7 (3955.1–46 956.1)[m]	6281.8 (3253.8–19 266.4)[l]	0.055[l]
Neopterin (pg/ml)	1817.6 (425.3–5715.5)[f]	634.6 (469.0–2267.5)[l]	<0.001[m]
IL-6 (pg/ml)	2.10 (0.70–20.70)[i]	1.40 (0.90–8.40)[l]	0.07[j]
IL-1β (pg/ml)	0.55 (0.50–0.60)[n]	0.50 (0.50–0.60)[o]	0.66[o]
TNF-α (pg/ml)	0.50 (0.20–7.20)[i]	0.40 (0.20–3.60)[l]	0.011[m]
MCP-1 (pg/ml)	903.7 (151.7–4056.8)[f]	731.2 (386.8–1066.1)[l]	0.29[l]
IP-10 (pg/ml)	935.1 (17.7–7006.0)[f]	552.3 (111.3–2164.0)[l]	0.004[l]

P values were computed by Wilcoxon signed-rank test. Percentages shown are valid percentage and exclude missing data. IL, interleukin; IP, interferon-γ-inducible protein 10; MCP, monocyte chemoattractant protein; S100B, S100 calcium-binding protein B; sCD163, soluble CD163; TNF, tumor necrosis factor.
[a]Data were available for 31 participants.
[b]$n = 28$
[c]$n = 16$
[d]$n = 30$
[e]$n = 31$
[f]$n = 27$
[g]$n = 24$
[h]$n = 22$
[i]$n = 21$
[j]$n = 14$
[k]$n = 10$
[l]$n = 17$
[m]$n = 20$
[n]$n = 13$
[o]$n = 11$.

months of cART (Table 2). As computed by the median percentage change, caudate and putamen volumes decreased by approximately 3%. The changes were significant after Holm–Bonferroni correction and were subsequently examined for relationships with baseline brain metabolites, plasma and CSF biomarkers, and monocyte subsets.

The TBM results can be visualized in Fig. 1. Briefly, TBM showed that the most significant change from baseline occurred bilaterally in the putamen (up to 5.2% atrophy in 24 months, $P < 5 \times 10^{-6}$, corrected), confirming FreeSurfer findings. Atrophy of the caudate was significant, although less striking at 2.5% ($P < 1.4 \times 10^{-4}$, corrected). In the thalamus, atrophy of approximately 4% was detected over 24 months ($P < 2 \times 10^{-4}$, corrected). Thalamic atrophy appears to be in regions representing the ventral posterior nucleus, pulvinar, lateral geniculate nucleus, and/or medial geniculate nucleus (individual nuclei cannot be distinguished without higher field strength and spatial resolution, so their identities were inferred from the observed locations of atrophy). The head of the hippocampus exhibited nearly 3% atrophy in 24 months ($P < 2 \times 10^{-4}$, corrected). Significant volumetric loss was also noted outside subcortical regions; for example, in the orbitofrontal cortex and the cingulate gyrus. Large portions of temporal white matter were observed to

Table 2. Regional brain volumes (mm^3, mean ± SD) at baseline and 24 months.

Brain region	Month 0 (baseline)	Month 24	*P*
Caudate nucleus[a]	7147.2 ± 867.7	7024.5 ± 890.3	0.006
Putamen[a]	11 364.3 ± 980.4	11 102.1 ± 1031.0	<0.001
Cerebral WM	434 475.2 ± 58 084.5	432 401.3 ± 57,357.4	0.07
Hippocampus	9185.4 ± 930.3	9219.2 ± 945.0	0.08
Cortical GM	459 051.0 ± 48 940.2	460 639.4 ± 46 801.2	0.13
Thalamus	15 206.8 ± 1496.8	15 169.2 ± 1425.9	0.40
Pallidum	3200.9 ± 430.4	3187.8 ± 405.2	0.38
Nucleus accumbens	1149.6 ± 163.0	1160.1 ± 275.3	0.51
Amygdala	2985.2 ± 337.5	2940.1 ± 443.1	0.48

P values were computed by Wilcoxon signed-rank test for related samples. GM, gray matter; WM, white matter.
[a]Significant after Holm–Bonferroni correction for multiple comparisons.

undergo atrophy of up to 3% ($P < 2 \times 10^{-6}$, corrected), along with the isthmus of the corpus callosum (2.5% atrophy; $P < 1 \times 10^{-4}$, corrected). In addition, CSF expansion was detected in sulcal regions.

Baseline clinical variables and regional brain volumetric change

Changes in caudate and putamen volumes did not correlate with age, years of education, baseline CD4$^+$ cell count, plasma viral load, CSF viral load, or mega-cART status. Suppression of plasma viral load below 50 copies/ml by week 4 ($n = 8$) was associated with a smaller decrease from M0 to M24 in caudate volume (median 0.66 vs. 3.1%; $P = 0.009$), and a trend toward lower putamen volume loss (1.9 vs. 3.5%; $P = 0.07$).

Baseline brain metabolites as predictors of regional brain volumetric change

Greater change (decrease) in putamen volume correlated with lower baseline Cho/creatine ($\rho = -0.43$, $P = 0.015$) and lower Glx/creatine ($\rho = -0.39$, $P = 0.027$) in frontal GM (Fig. 2). The results do not survive Holm–Bonferroni correction for comparisons involving four metabolite ratios, four MRS voxel locations, and two regional volumes. Brain metabolite ratios at baseline did not relate to reduced caudate volume.

Substance use, co-infections, and regional brain volumetric change

To examine the possible confounding effects of substance use on our results, we compared percentage volume changes of caudate and putamen between participants

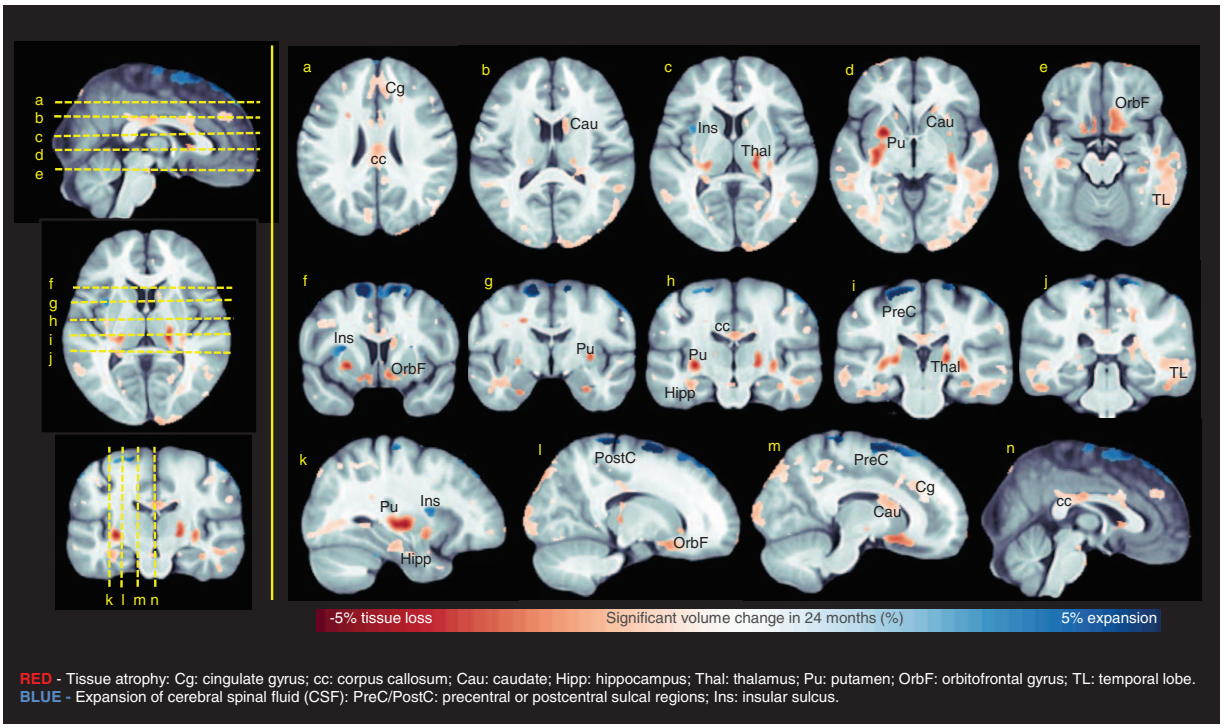

Fig. 1. Significant changes in regional brain volumes at 24 months post-baseline. Two-dimensional representation of volumetric changes identified by tensor-based morphometry (TBM). Warmer colors indicate greater atrophy.

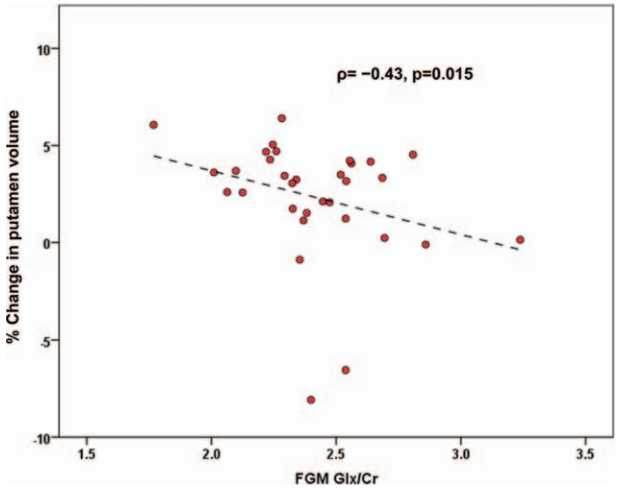

Fig. 2. Putamen volume change at 24 months post-baseline plotted against baseline Glx/(Cr) in frontal gray matter (FGM). Glx = glutamate (Glu) + glutamine (Gln); Cr = creatine; percentage volume change = (M0 − M24) × 100/M0, where M0 = volume at month 0 and M24 = volume at month 24; and ρ is the Spearman correlation coefficient. Putamen volumes were obtained by processing T1-weighted magnetic resonance imaging data with the FreeSurfer longitudinal pipeline.

who had used illicit substances during the 4 months preceding enrollment ($n = 10$) and those who had not ($n = 21$). The groups did not differ in either putamen (Mann–Whitney $P = 0.72$) or caudate ($P = 0.35$) volume loss. Additionally, we assessed caudate and putamen atrophy from M0 to M24 separately in the users and nonusers. For the putamen, P values of 0.013 and 0.012 for users and nonusers, respectively, revealed volumetric changes in both groups (less significant than in the combined sample because of reduced power). Similarly, caudate volume loss was comparable between users ($P = 0.059$) and nonusers ($P = 0.063$).

Volumetric loss in the putamen and caudate remained essentially unaltered when the three cases of co-infection with syphilis, gonorrhoea, or hepatitis C at baseline were excluded from analyses.

Plasma and cerebrospinal fluid biomarkers and monocyte subsets

Exploratory analyses examined baseline values of plasma and CSF biomarkers as predictors of percentage volume changes of the caudate and putamen. No significant correlations were found. Associations were also assessed between the volumetric changes and baseline blood monocyte subpopulations, including those expressing CCR2, CCR5, CX3CR1, PSGL-1, and CD163. Greater decrease in caudate volume correlated with higher total frequency and density [mean fluorescence intensity (MFI)] of PSGL-1-expressing monocytes at baseline ($\rho = 0.67$, $P = 0.017$; and $\rho = 0.60$, $P = 0.038$, respectively). Putamen volume decrease correlated positively with the baseline frequency ($\rho = 0.61$, $P = 0.037$) and density ($\rho = 0.65$, $P = 0.022$) of PSGL-1-expressing inflammatory monocytes. Volumetric associations with PSGL-1-expressing monocytes are plotted in Fig. 3.

Discussion

Contrary to expectations, AHI participants demonstrated decreased volumes of caudate and putamen after 2 years of cART. The finding that brain injury may occur despite very early implementation of therapy is somewhat surprising, given the anticipated neuroprotective effects of acutely administered cART. However, HIV invasion of the CNS within 8 days of exposure [41] and CNS inflammation during AHI [41] constitute indirect evidence that the impact of HIV on the brain is almost immediate and may compete with mitigating effects of concomitant cART initiation. Our results are bolstered by data from separate cohorts indicating early brain damage and preferential susceptibility of the putamen during PHI [11,56]. Impaired cognition seen in a subset of SEARCH010/RV254 participants after 6 months of treatment [57] suggests that brain injury may be incompletely ameliorated. Moreover, consistent with our findings, the cognitive deficits were manifested in domains in which basal ganglia play crucial roles (psychomotor speed, fine motor skills, and executive functioning [57–59]). Reduced putamen volume in PHI has been correlated with psychomotor slowing [56], and basal ganglia reductions in chronic HIV disease are associated with motor [60] and executive [61] dysfunction.

The decreases of about 3% in putamen and caudate volumes over 2 years, or annual atrophy rates of 1.5% which we note are greater than the 0.63%/year rate reported even in untreated PHI [30], should be compared with normal age-related loss. Published rates of brain atrophy in healthy individuals are inconsistent [62]. Cross-sectional studies may not accurately characterize normal change [63,64], and many longitudinal studies, in addressing brain development or aging, overlook younger adults. Research on older adults typically focuses on global and medial temporal lobe atrophy in the context of aging-related dementia, with consequent neglect of other regions [63]. A 5-year study of healthy individuals (baseline age 20–77 years) measured respective annual atrophy rates of 0.83 and 0.73% for the caudate and putamen, independently of age [65]. In a different, similarly aged cohort, caudate and putamen shrinkage over 2 years was 0.44 and 0.47% (i.e. negligible) [66]. The decreases we observed in putamen and caudate volumes most likely reflect atrophy due to HIV (or to neurotoxic effects of cART), although this remains speculative in the absence of an HIV-uninfected Thai comparison group.

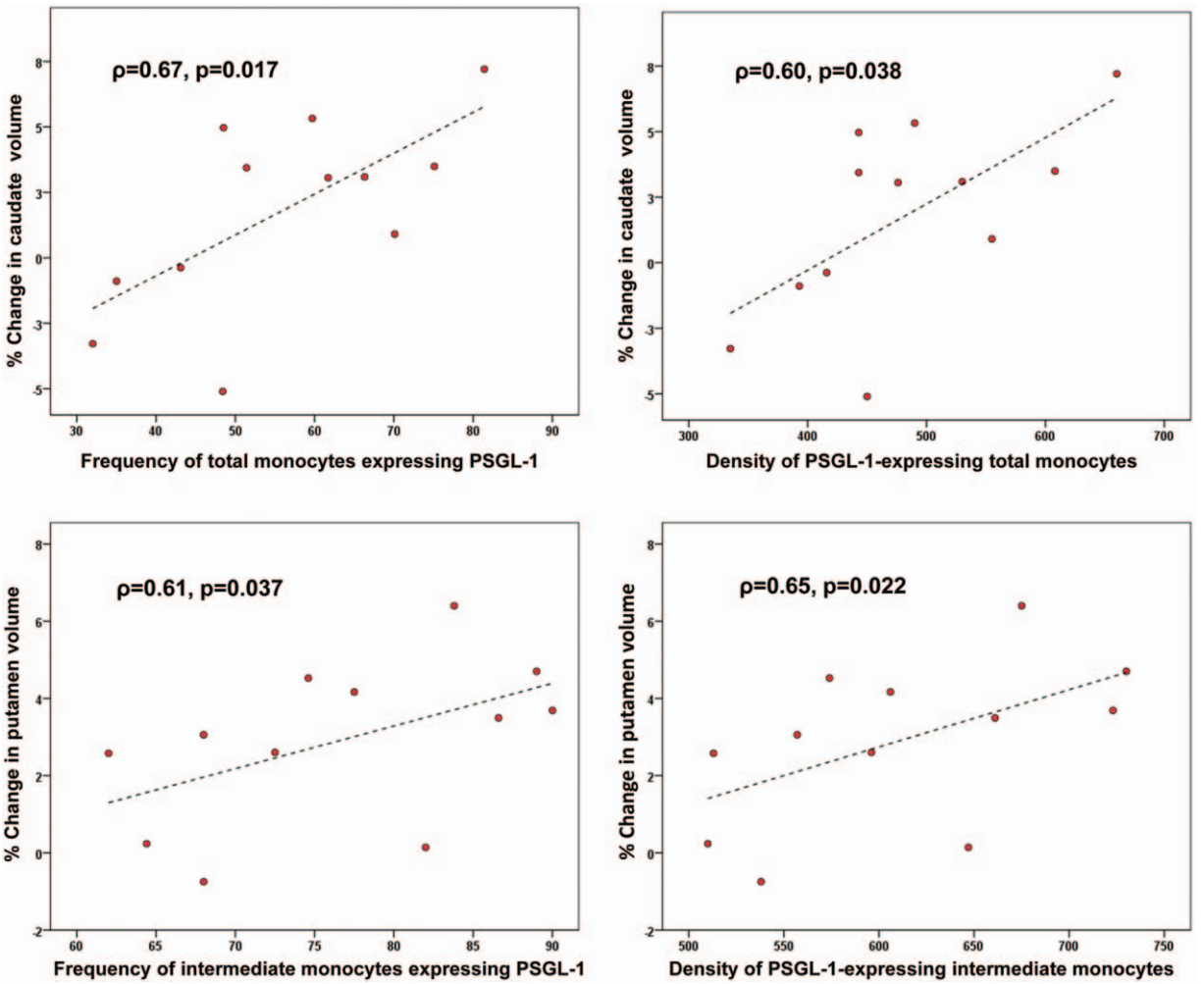

Fig. 3. Caudate and putamen volume changes at 24 months post-baseline plotted against frequencies and densities of circulating intermediate/inflammatory ($CD14^+CD16^+$) and total monocytes expressing P-selectin glycoprotein ligand-1 (PSGL-1). Percentage volume change = (M0 − M24) × 100/M0, where M0 = volume at month 0 and M24 = volume at month 24; ρ is the Spearman correlation coefficient. T1-weighted magnetic resonance imaging data were processed with the FreeSurfer longitudinal pipeline to obtain regional brain volumes.

Caudate and putamen atrophy was lowest in participants who achieved plasma HIV RNA below 50 copies/ml by week 4. The trend association observed between mega-cART and rapidity of viral suppression is supported by previous observations of the SEARCH 010/RV254 cohort [67] and by neurocognitive improvement linked to maraviroc-intensified cART [68]. Taken together, these findings indicate that cART intensification by raltegravir and maraviroc should be further examined for its ability to preserve brain integrity in HIV-infected individuals.

A potential limitation of morphometric MRI studies is the reliability of regional brain volume estimates. Longitudinal investigations of atrophy are facilitated by automated segmentation software, but confounded by multiple factors including variability due to data processing techniques. Gunter *et al.* [69] conducted a careful examination of sources of error in a study of semiautomated methods for computing brain volume loss. Volunteers aged 23–45 years were scanned every 6 weeks over a 5-month period to gauge errors inherent in the measurement process. With atrophy assumed to be imperceptible, image processing accounted for only 1/5 to 1/2 of test–retest variability [69]. Other variations reflected MRI acquisition differences (head position, motion, etc.) or real changes (e.g. from hydration effects [69,70]), which, together with variability due to quantification methods, make 'true' rates of atrophy elusive [69]. Recent versions of FreeSurfer are competitive with gold standard manual measurements in cognitively normal and impaired individuals [71], and FreeSurfer was validated for subcortical volumetry in HIV [72]. Importantly, for healthy young volunteers

(aged 26–31 years) scanned repeatedly over 31 days (20 sessions; 2 scans per session), FreeSurfer's intersession volumetric variability did not exceed intrasession variability for the caudate, putamen, or any structure, except lateral ventricles [73] (intrasession variability is presumably unaffected by biological change). The reliability and consistency of FreeSurfer volume estimates in health and disease [72,74–79] impart confidence in our findings, which were confirmed by TBM analyses.

Decreased astrocytic uptake and glutamate metabolism is a major contributing factor in excitotoxic neuronal death linked to cognitive impairment in HIV [80,81]. We observed relationships between putamen atrophy and lower baseline Cho/creatine and Glx/creatine in frontal gray matter, which did not, however, overcome correction for multiple comparisons. Our ability to identify such associations may have been constrained by the modest sample size. The analyses of monocyte inflammatory markers also were exploratory and not corrected for multiple comparisons. However, the link between baseline monocyte expression of PSGL-1 and basal ganglia shrinkage suggests that increased trafficking of HIV-infected monocytes into the brain in AHI may play a causative role in subsequent atrophy. PSGL-1 promotes leukocyte trafficking across the blood–brain barrier (BBB) during inflammation by tethering the leukocytes to endothelial surfaces of blood vessels [82,83]. The intermediate/inflammatory $CD14^+CD16^+$ monocyte subset, in particular, appears to be involved in putamen atrophy. CD16-expressing monocytes are highly susceptible to HIV infection [84], selectively transmigrate across the BBB [84], and preferentially harbor the virus in cART-treated individuals [85]. New findings indicate that PSGL-1 promotes T-cell immune exhaustion, and it has also become evident that migration-independent functions of PSGL-1 in myeloid cells lead to immune activation and increased MCP-1 secretion through a mammalian target of rapamycin (mTOR) pathway [86]. Collectively, these findings provide clues to mechanisms associated with brain atrophy that warrant further investigation.

As CSF S100B and monocyte data were available only for participant subsets, our analyses of brain volumetric change in relation to baseline S100B and monocyte subsets had limited power. The sample size did not allow statistical adjustments for several known modifiers of brain aging, either adverse (e.g. vascular risk factors and stress) or beneficial (educational level, aerobic fitness) [62], which could affect brain volumes in this cohort. Comparison with normal brain alterations was hampered by the lack of an HIV-uninfected Thai comparison group. Nevertheless, likely confounding factors such as substance use and sexually transmitted diseases (STDs) did not appear to influence our results. STD prevalence was below 6% and had no effect. The relatively low rate of illicit substance use in the SEARCH010/RV254 cohort [57] distinguishes it from other HIV studies that may have been confounded by drug or alcohol consumption (reviewed by Zahr [87]). Recreational substance use data were self-reported, available only at M0, and during the period of our study, not systematically collected, which limited their usefulness. However, individuals recruited into the cohort reported no history of substance use judged severe enough to compromise patient care (as evidenced by viral suppression by week 36 in 100% of the sample). Sensitivity analyses confirmed that illicit substance use in the 4 months prior to baseline did not affect atrophy of the caudate or putamen.

A unique strength of the SEARCH010/RV254 study is its well characterized cohort, a significant proportion of which initiates cART during Fiebig I/II, permitting assessment of the earliest phase of the disease and the impact of immediate treatment. This eliminates what usually is a major source of uncertainty, the duration of infection, and minimizes the occurrence of pre-cART damage – a critical obstacle in determining whether cART is protective.

Conclusions

Participants enrolled during AHI exhibited progressive brain atrophy 2 years after infection, despite very early initiation of cART. Longitudinal assessment of HIV-uninfected Thai individuals is required to determine whether the volumetric decline is steeper than in healthy controls. Intensification of cART by maraviroc and raltegravir may inhibit brain atrophy by promoting faster viral suppression. Caudate and putamen volume loss is supported by a plausible link to early expansion of PSGL-1-expressing monocytes, particularly the intermediate/inflammatory subpopulation. Therapeutic strategies targeting viral production in PSGL-1 monocytes may reduce HIV-CNS invasion and eventual brain injury.

Acknowledgements

We thank our study participants and staff from the Thai Red Cross AIDS Research Centre and the Silom Community Clinic in Bangkok for their contributions, and Ms Shayanne Martin for her helpful suggestions and assistance with data collection.

Author contributions: K.J.K. supervised FreeSurfer MRI data processing, performed statistical analyses and data interpretation, prepared tables and figures, and drafted the manuscript. N.J. conducted TBM data analyses, prepared a figure, and helped to edit the manuscript. N.S. supervised neuroimaging data acquisition and processed the MRS data. K.B. assisted with clinical data collection.

P.C. was the on-site neurologist who conducted neurological assessment and clinical follow-up. M.P. conducted the MRI/MRS scanning. N.D. was the radiologist in charge of protocol for MRI/MRS. E.L. conducted cytokine measurements. L.C.N. supervised cytokine measurement and helped to edit the manuscript. K.M.C. performed FreeSurfer processing of MRI data. R.P. contributed to data interpretation and manuscript editing. L.J. performed HIV serology and measured CSF HIV RNA. S.K. measured CSF S100B levels. J.A and S.S. participated in study conception and design, data interpretation, and manuscript editing. V.V. participated in study conception and design, data interpretation, and writing and editing of the manuscript. All authors read and approved the final manuscript.

Funding: This study was supported by NIH grants R01-MH-113560, R01-MH-10414, R01-AG-059874, R21-MH0-86341, K24-MH-098759 and R01-MH-095613; and by the US Military HIV Research Program through its cooperative agreement with the Henry M. Jackson Foundation for the Advancement of Military Medicine, Inc. (W81XWH-07-2-0067, W81XWH-11-2-0174). The views, opinions, and/or findings contained in this report are those of the authors and should not be construed as an official Department of the Army position, policy or decision unless so designated by other documentation. In addition, the content of this manuscript is solely the responsibility of the authors and does not necessarily represent the official views of the U.S. Department of Defense, National Institutes of Health, Department of Health and Human Services, or the United States government and the Thai Red Cross AIDS Research Centre.

Conflicts of interest

There are no conflicts of interest.

References

1. Nir TM, Jahanshad N, Ching CRK, Cohen RA, Harezlak J, Schifitto G, *et al*. **Progressive brain atrophy in chronically infected and treated HIV+ individuals.** *J Neurovirol* 2019; **25**:342–353.
2. Harezlak J, Buchthal S, Taylor M, Schifitto G, Zhong J, Daar E, *et al*. **Persistence of HIV-associated cognitive impairment, inflammation, and neuronal injury in era of highly active antiretroviral treatment.** *AIDS* 2011; **25**:625–633.
3. Ances BM, Ortega M, Vaida F, Heaps J, Paul R. **Independent effects of HIV, aging, and HAART on brain volumetric measures.** *J Acquir Immune Defic Syndr* 2012; **59**:469–477.
4. Melrose RJ, Tinaz S, Castelo JM, Courtney MG, Stern CE. **Compromised fronto-striatal functioning in HIV: an fMRI investigation of semantic event sequencing. Behav.** *Brain Res* 2008; **188**:337–347.
5. Ipser JC, Brown GG, Bischoff-Grethe A, Connolly CG, Ellis RJ, Heaton RK, *et al*. **HIV infection is associated with attenuated frontostriatal intrinsic connectivity: a preliminary study.** *J Int Neuropsychol Soc* 2015; **21**:203–213.
6. Baker LM, Cooley SA, Cabeen RP, Laidlaw DH, Joska JA, Hoare J, *et al*. **Topological organization of whole-brain white matter in HIV infection.** *Brain Connect* 2017; **7**:115–122.
7. Cohen RA, Harezlak J, Schifitto G, Hana G, Clark U, Gongvatana A, *et al*. **Effects of nadir CD4 count and duration of human immunodeficiency virus infection on brain volumes in the highly active antiretroviral therapy era.** *J Neurovirol* 2010; **16**:25–32.
8. Jernigan TL, Archibald SL, Fennema-Notestine C, Taylor MJ, Theilmann RJ, Julaton MD, *et al*. **Clinical factors related to brain structure in HIV: the CHARTER study.** *J Neurovirol* 2011; **17**:248–257.
9. Gongvatana A, Schweinsburg BC, Taylor MJ, Theilmann RJ, Letendre SL, Alhassoon OM, *et al*. **White matter tract injury and cognitive impairment in human immunodeficiency virus-infected individuals.** *J Neurovirol* 2009; **15**:187–195.
10. Valcour V, Sithinamsuwan P, Letendre S, Ances B. **Pathogenesis of HIV in the central nervous system.** *Curr HIV/AIDS Rep* 2011; **8**:54–61.
11. Ragin AB, Du H, Ochs R, Wu Y, Sammet CL, Shoukry A, *et al*. **Structural brain alterations can be detected early in HIV infection.** *Neurology* 2012; **79**:2328–2334.
12. Ragin AB, Wu Y, Gao Y, Keating S, Du H, Sammet C, *et al*. **Brain alterations within the first 100 days of HIV infection.** *Ann Clin Transl Neurol* 2015; **2**:12–21.
13. Cao B, Kong X, Kettering C, Yu P, Ragin A. **Determinants of HIV-induced brain changes in three different periods of the early clinical course: a data mining analysis.** *Neuroimage Clin* 2015; **9**:75–82.
14. Kelley CF, Kitchen CM, Hunt PW, Rodriguez B, Hecht FM, Kitahata M, *et al*. **Incomplete peripheral CD4+ cell count restoration in HIV-infected patients receiving long-term antiretroviral treatment.** *Clin Infect Dis* 2009; **48**:787–794.
15. Le T, Wright EJ, Smith DM, He W, Catano G, Okulicz JF, *et al*. **Enhanced CD4+ T-cell recovery with earlier HIV-1 antiretroviral therapy.** *N Engl J Med* 2013; **368**:218–230.
16. Abdulle S, Mellgren A, Brew BJ, Cinque P, Hagberg L, Price RW, *et al*. **CSF neurofilament protein (NFL): a marker of active HIV-related neurodegeneration.** *J Neurol* 2007; **254**:1026–1032.
17. Peluso MJ, Meyerhoff DJ, Price RW, Peterson J, Lee E, Young AC, *et al*. **Cerebrospinal fluid and neuroimaging biomarker abnormalities suggest early neurological injury in a subset of individuals during primary HIV infection.** *J Infect Dis* 2013; **207**:1703–1712.
18. Peluso MJ, Valcour V, Ananworanich J, Sithinamsuwan P, Chalermchai T, Fletcher JL, *et al*. **Absence of cerebrospinal fluid signs of neuronal injury before and after immediate antiretroviral therapy in acute HIV infection.** *J Infect Dis* 2015; **212**:1759–1767.
19. Jain V, Hartogensis W, Bacchetti P, Hunt PW, Hatano H, Sinclair E, *et al*. **Antiretroviral therapy initiated within 6 months of HIV infection is associated with lower T-cell activation and smaller HIV reservoir size.** *J Infect Dis* 2013; **208**:1202–1211.
20. Ananworanich J, Chomont N, Eller LA, Kroon E, Tovanabutra S, Bose M, *et al*. **HIV DNA set point is rapidly established in acute HIV infection and dramatically reduced by early ART.** *EBioMedicine* 2016; **11**:68–72.
21. Lee TH, Sheppard HW, Reis M, Dondero D, Osmond D, Busch MP. **Circulating HIV-1-infected cell burden from seroconversion to AIDS: importance of postseroconversion viral load on disease course.** *J Acquir Immune Defic Syndr* 1994; **7**:381–388.
22. Williams JP, Hurst J, Stohr W, Robinson N, Brown H, Fisher M, *et al*. **HIV-1 DNA predicts disease progression and posttreatment virological control.** *Elife* 2014; **3**:e03821.
23. Li JZ, Etemad B, Ahmed H, Aga E, Bosch RJ, Mellors JW, *et al*. **The size of the expressed HIV reservoir predicts timing of viral rebound after treatment interruption.** *AIDS* 2016; **30**:343–353.
24. Ndhlovu LC, D'Antoni ML, Ananworanich J, Byron MM, Chalermchai T, Sithinamsuwan P, *et al*. **Loss of CCR2 expressing nonclassical monocytes are associated with cognitive impairment in antiretroviral therapy-naive HIV-infected Thais.** *J Neuroimmunol* 2015; **288**:25–33.
25. Burdo TH, Lentz MR, Autissier P, Krishnan A, Halpern E, Letendre S, *et al*. **Soluble CD163 made by monocyte/macrophages is a novel marker of HIV activity in early and chronic infection prior to and after antiretroviral therapy.** *J Infect Dis* 2011; **204**:154–163.

26. D'Antoni ML, Byron MM, Chan P, Sailasuta N, Sacdalan C, Sithinamsuwan P, *et al*. **Normalization of soluble CD163 levels after institution of antiretroviral therapy during acute HIV infection tracks with fewer neurological abnormalities.** *J Infect Dis* 2018; **218**:1453–1463.
27. Davis LE, Hjelle BL, Miller VE, Palmer DL, Llewellyn AL, Merlin TL, *et al*. **Early viral brain invasion in iatrogenic human immunodeficiency virus infection.** *Neurology* 1992; **42**:1736–1739.
28. Paci P, Martini F, Bernaschi M, D'Offizi G, Castiglione F. **Timely HAART initiation may pave the way for a better viral control.** *BMC Infect Dis* 2011; **11**:56.
29. Clifford KM, Samboju V, Cobigo Y, Milanini B, Marx GA, Hellmuth JM, *et al*. **Progressive brain atrophy despite persistent viral suppression in HIV patients older than 60 years.** *J Acquir Immune Defic Syndr* 2017; **76**:289–297.
30. Sanford R, Ances BM, Meyerhoff DJ, Price RW, Fuchs D, Zetterberg H, *et al*. **Longitudinal trajectories of brain volume and cortical thickness in treated and untreated primary HIV infection.** *Clin Infect Dis* 2018; **67**:1697–1704.
31. Sanford R, Fellows LK, Ances BM, Collins DL. **Association of brain structure changes and cognitive function with combination antiretroviral therapy in HIV-positive individuals.** *JAMA Neurol* 2018; **75**:72–79.
32. Cole JH, Caan MWA, Underwood J, De Francesco D, van Zoest RA, Wit F, *et al*. **No evidence for accelerated aging-related brain pathology in treated human immunodeficiency virus: longitudinal neuroimaging results from the Comorbidity in Relation to AIDS (COBRA) Project.** *Clin Infect Dis* 2018; **66**:1899–1909.
33. Hua X, Boyle CP, Harezlak J, Tate DF, Yiannoutsos CT, Cohen R, *et al*. **Disrupted cerebral metabolite levels and lower nadir CD4 + counts are linked to brain volume deficits in 210 HIV-infected patients on stable treatment.** *Neuroimage Clin* 2013; **3**:132–142.
34. Gongvatana A, Correia S, Dunsiger S, Gauthier L, Devlin KN, Ross S, *et al*. **Plasma cytokine levels are related to brain volumes in HIV-infected individuals.** *J Neuroimmune Pharmacol* 2014; **9**:740–750.
35. Valcour VG, Ananworanich J, Agsalda M, Sailasuta N, Chalermchai T, Schuetz A, *et al*. **HIV DNA reservoir increases risk for cognitive disorders in cART-naive patients.** *PLoS One* 2013; **8**:e70164.
36. Kallianpur KJ, Shikuma C, Kirk GR, Shiramizu B, Valcour V, Chow D, *et al*. **Peripheral blood HIV DNA is associated with atrophy of cerebellar and subcortical gray matter.** *Neurology* 2013; **80**:1792–1799.
37. Shive CL, Jiang W, Anthony DD, Lederman MM. **Soluble CD14 is a nonspecific marker of monocyte activation.** *AIDS* 2015; **29**:1263–1265.
38. Tenorio AR, Zheng Y, Bosch RJ, Krishnan S, Rodriguez B, Hunt PW, *et al*. **Soluble markers of inflammation and coagulation but not T-cell activation predict non-AIDS-defining morbid events during suppressive antiretroviral treatment.** *J Infect Dis* 2014; **210**:1248–1259.
39. Green AJ, Harvey RJ, Thompson EJ, Rossor MN. **Increased S100beta in the cerebrospinal fluid of patients with frontotemporal dementia.** *Neurosci Lett* 1997; **235**:5–8.
40. Petzold A, Jenkins R, Watt HC, Green AJ, Thompson EJ, Keir G, *et al*. **Cerebrospinal fluid S100B correlates with brain atrophy in Alzheimer's disease.** *Neurosci Lett* 2003; **336**:167–170.
41. Valcour V, Chalermchai T, Sailasuta N, Marovich M, Lerdlum S, Suttichom D, *et al*. **Central nervous system viral invasion and inflammation during acute HIV infection.** *J Infect Dis* 2012; **206**:275–282.
42. Sailasuta N, Ross W, Ananworanich J, Chalermchai T, DeGruttola V, Lerdlum S, *et al*. **Change in brain magnetic resonance spectroscopy after treatment during acute HIV infection.** *PLoS One* 2012; **7**:e49272.
43. Ananworanich J, Schuetz A, Vandergeeten C, Sereti I, de Souza M, Rerknimitr R, *et al*. **Impact of multitargeted antiretroviral treatment on gut T cell depletion and HIV reservoir seeding during acute HIV infection.** *PLoS One* 2012; **7**:e33948.
44. De Souza MS, Phanuphak N, Pinyakorn S, Trichavaroj R, Pattanachaiwit S, Chomchey N, *et al*. **Impact of nucleic acid testing relative to antigen/antibody combination immunoassay on the detection of acute HIV infection.** *AIDS* 2015; **29**:793–800.
45. Fiebig EW, Wright DJ, Rawal BD, Garrett PE, Schumacher RT, Peddada L, *et al*. **Dynamics of HIV viremia and antibody seroconversion in plasma donors: implications for diagnosis and staging of primary HIV infection.** *AIDS* 2003; **17**:1871–1879.
46. Price RW, Yiannoutsos CT, Clifford DB, Zaborski L, Tselis A, Sidtis JJ, *et al*. **Neurological outcomes in late HIV infection: adverse impact of neurological impairment on survival and protective effect of antiviral therapy. AIDS Clinical Trial Group and Neurological AIDS Research Consortium study team.** *AIDS* 1999; **13**:1677–1685.
47. Schirmer T, Auer DP. **On the reliability of quantitative clinical magnetic resonance spectroscopy of the human brain.** *NMR Biomed* 2000; **13**:28–36.
48. Reuter M, Schmansky NJ, Rosas HD, Fischl B. **Within-subject template estimation for unbiased longitudinal image analysis.** *Neuroimage* 2012; **61**:1402–1418.
49. Fischl B, Salat DH, Busa E, Albert M, Dieterich M, Haselgrove C, *et al*. **Whole brain segmentation: automated labeling of neuroanatomical structures in the human brain.** *Neuron* 2002; **33**:341–355.
50. McCarthy CS, Ramprashad A, Thompson C, Botti JA, Coman IL, Kates WR. **A comparison of FreeSurfer-generated data with and without manual intervention.** *Front Neurosci* 2015; **9**:379.
51. Ellis RJ, Badiee J, Vaida F, Letendre S, Heaton RK, Clifford D, *et al*. **CD4 nadir is a predictor of HIV neurocognitive impairment in the era of combination antiretroviral therapy.** *AIDS* 2011; **25**:1747–1751.
52. Burdo TH, Weiffenbach A, Woods SP, Letendre S, Ellis RJ, Williams KC. **Elevated sCD163 in plasma but not cerebrospinal fluid is a marker of neurocognitive impairment in HIV infection.** *AIDS* 2013; **27**:1387–1395.
53. Jalbert E, Shikuma CM, Ndhlovu LC, Barbour JD. **Sequential staining improves detection of CCR2 and CX3CR1 on monocytes when simultaneously evaluating CCR5 by multicolor flow cytometry.** *Cytometry A* 2013; **83**:280–286.
54. Holm S. **A simple sequentially rejective multiple test procedure.** *Scand J Stat* 1979; **6**:65–70.
55. Avants BB, Tustison NJ, Song G, Cook PA, Klein A, Gee JC. **A reproducible evaluation of ANTs similarity metric performance in brain image registration.** *Neuroimage* 2011; **54**:2033–2044.
56. Wright PW, Pyakurel A, Vaida FF, Price RW, Lee E, Peterson J, *et al*. **Putamen volume and its clinical and neurological correlates in primary HIV infection.** *AIDS* 2016; **30**:1789–1794.
57. Kore I, Ananworanich J, Valcour V, Fletcher JL, Chalermchai T, Paul R, *et al*. **Neuropsychological impairment in acute HIV and the effect of immediate antiretroviral therapy.** *J Acquir Immune Defic Syndr* 2015; **70**:393–399.
58. DeLong MR, Alexander GE, Georgopoulos AP, Crutcher MD, Mitchell SJ, Richardson RT. **Role of basal ganglia in limb movements.** *Hum Neurobiol* 1984; **2**:235–244.
59. Grahn JA, Parkinson JA, Owen AM. **The role of the basal ganglia in learning and memory: neuropsychological studies.** *Behav Brain Res* 2009; **199**:53–60.
60. Kuper M, Rabe K, Esser S, Gizewski ER, Husstedt IW, Maschke M, *et al*. **Structural gray and white matter changes in patients with HIV.** *J Neurol* 2011; **258**:1066–1075.
61. Correa DG, Zimmermann N, Netto TM, Tukamoto G, Ventura N, de Castro Bellini Leite S, *et al*. **Regional cerebral gray matter volume in HIV-positive patients with executive function deficits.** *J Neuroimaging* 2016; **26**:450–457.
62. Raz N, Rodrigue KM. **Differential aging of the brain: patterns, cognitive correlates and modifiers.** *Neurosci Biobehav Rev* 2006; **30**:730–748.
63. Raz N, Ghisletta P, Rodrigue KM, Kennedy KM, Lindenberger U. **Trajectories of brain aging in middle-aged and older adults: regional and individual differences.** *Neuroimage* 2010; **51**:501–511.
64. Raz N, Lindenberger U. **Only time will tell: cross-sectional studies offer no solution to the age-brain-cognition triangle: comment on Salthouse (2011).** *Psychol Bull* 2011; **137**:790–795.
65. Raz N, Rodrigue KM, Kennedy KM, Head D, Gunning-Dixon F, Acker JD. **Differential aging of the human striatum: longitudinal evidence.** *AJNR Am J Neuroradiol* 2003; **24**:1849–1856.

66. Persson N, Ghisletta P, Dahle CL, Bender AR, Yang Y, Yuan P, *et al*. **Regional brain shrinkage over two years: individual differences and effects of pro-inflammatory genetic polymorphisms.** *Neuroimage* 2014; **103**:334–348.
67. Ananworanich J, Chomont N, Fletcher JL, Pinyakorn S, Schuetz A, Sereti I, *et al*. **Markers of HIV reservoir size and immune activation after treatment in acute HIV infection with and without raltegravir and maraviroc intensification.** *J Virus Erad* 2015; **1**:116–122.
68. Gates TM, Cysique LA, Siefried KJ, Chaganti J, Moffat KJ, Brew BJ. **Maraviroc-intensified combined antiretroviral therapy improves cognition in virally suppressed HIV-associated neurocognitive disorder.** *AIDS* 2016; **30**:591–600.
69. Gunter JL, Shiung MM, Manduca A, Jack CR Jr. **Methodological considerations for measuring rates of brain atrophy.** *J Magn Reson Imaging* 2003; **18**:16–24.
70. Duning T, Kloska S, Steinstrater O, Kugel H, Heindel W, Knecht S. **Dehydration confounds the assessment of brain atrophy.** *Neurology* 2005; **64**:548–550.
71. Clerx L, Gronenschild EH, Echavarri C, Verhey F, Aalten P, Jacobs HI. **Can FreeSurfer compete with manual volumetric measurements in Alzheimer's disease?** *Curr Alzheimer Res* 2015; **12**:358–367.
72. Dewey J, Hana G, Russell T, Price J, McCaffrey D, Harezlak J, *et al*. **Reliability and validity of MRI-based automated volumetry software relative to auto-assisted manual measurement of subcortical structures in HIV-infected patients from a multisite study.** *Neuroimage* 2010; **51**:1334–1344.
73. Maclaren J, Han Z, Vos SB, Fischbein N, Bammer R. **Reliability of brain volume measurements: a test-retest dataset.** *Sci Data* 2014; **1**:140037.
74. Keller SS, Gerdes JS, Mohammadi S, Kellinghaus C, Kugel H, Deppe K, *et al*. **Volume estimation of the thalamus using freesurfer and stereology: consistency between methods.** *Neuroinformatics* 2012; **10**:341–350.
75. Cherbuin N, Anstey KJ, Reglade-Meslin C, Sachdev PS. **In vivo hippocampal measurement and memory: a comparison of manual tracing and automated segmentation in a large community-based sample.** *PLoS One* 2009; **4**:e5265.
76. Morey RA, Petty CM, Xu Y, Hayes JP, Wagner HR 2nd, Lewis DV, *et al*. **A comparison of automated segmentation and manual tracing for quantifying hippocampal and amygdala volumes.** *Neuroimage* 2009; **45**:855–866.
77. Pardoe HR, Pell GS, Abbott DF, Jackson GD. **Hippocampal volume assessment in temporal lobe epilepsy: how good is automated segmentation?** *Epilepsia* 2009; **50**:2586–2592.
78. Shen L, Saykin AJ, Kim S, Firpi HA, West JD, Risacher SL, *et al*. **Comparison of manual and automated determination of hippocampal volumes in MCI and early AD.** *Brain Imaging Behav* 2010; **4**:86–95.
79. Tae WS, Kim SS, Lee KU, Nam EC, Kim KW. **Validation of hippocampal volumes measured using a manual method and two automated methods (FreeSurfer and IBASPM) in chronic major depressive disorder.** *Neuroradiology* 2008; **50**:569–581.
80. Sardar AM, Hutson PH, Reynolds GP. **Deficits of NMDA receptors and glutamate uptake sites in the frontal cortex in AIDS.** *Neuroreport* 1999; **10**:3513–3515.
81. Vazquez-Santiago FJ, Noel RJ Jr, Porter JT, Rivera-Amill V. **Glutamate metabolism and HIV-associated neurocognitive disorders.** *J Neurovirol* 2014; **20**:315–331.
82. Kerfoot SM, Kubes P. **Overlapping roles of P-selectin and alpha 4 integrin to recruit leukocytes to the central nervous system in experimental autoimmune encephalomyelitis.** *J Immunol* 2002; **169**:1000–1006.
83. Ley K, Laudanna C, Cybulsky MI, Nourshargh S. **Getting to the site of inflammation: the leukocyte adhesion cascade updated.** *Nat Rev Immunol* 2007; **7**:678–689.
84. Williams DW, Eugenin EA, Calderon TM, Berman JW. **Monocyte maturation, HIV susceptibility, and transmigration across the blood brain barrier are critical in HIV neuropathogenesis.** *J Leukoc Biol* 2012; **91**:401–415.
85. Ellery PJ, Tippett E, Chiu YL, Paukovics G, Cameron PU, Solomon A, *et al*. **The CD16+ monocyte subset is more permissive to infection and preferentially harbors HIV-1 in vivo.** *J Immunol* 2007; **178**:6581–6589.
86. Tinoco R, Otero DC, Takahashi AA, Bradley LM. **PSGL-1: a new player in the immune checkpoint landscape.** *Trends Immunol* 2017; **38**:323–335.
87. Zahr NM. **The aging brain with HIV infection: effects of alcoholism or hepatitis C comorbidity.** *Frontiers Aging Neurosci* 2018; **10**:56.